

RECEIVED  
FEB 24 2000  
OPTICS

## Three-Dimensional Control of Light in a Two-Dimensional Photonic Crystal Slab

Edmond Chow<sup>1</sup>, S.Y. Lin<sup>1</sup>, S.G. Johnson<sup>2</sup>, P.R. Villeneuve<sup>2</sup>, J.D. Joannopoulos<sup>2</sup>, J.R. Wendt<sup>1</sup>, G.A. Vawter<sup>1</sup>, W. Zubrzycki<sup>1</sup>, H. Hou<sup>1</sup> and A. A. Allerman<sup>1</sup>

<sup>1</sup>Sandia National Laboratories, P.O. Box 5800, Albuquerque, NM 87185

<sup>2</sup>Department of Physics, Massachusetts Institute of Technology, Cambridge, MA 02139

\* H.Hou is currently at Emcore.

A two-dimensional (2D) photonic crystal is an attractive alternative and complementary to its 3D counterpart [1-5], due to fabrication simplicity. A 2D crystal, however, confines light only in the 2D plane [6], but not in the third direction, the  $z$ -direction. Earlier experiments show that such a 2D system can exist [7-10], providing that the boundary effect in  $z$ -direction is negligible and that light is collimated in the 2D plane. Nonetheless, the usefulness of such 2D crystals is limited because they are incapable of guiding light in  $z$ -direction, which leads to diffraction loss. This drawback presents a major obstacle for realizing low-loss 2D crystal waveguides, bends and thresholdless lasers. A recent theoretical calculation, though, suggests a novel way to eliminate such a loss with a 2D photonic crystal slab [11,12]. The concept of a lightcone is introduced as a criterion for fully guiding and controlling light. Although the leaky modes of a crystal slab have been studied [13], there have until now no experimental reports on probing its guided modes and band gaps.

In this paper, a waveguide-coupled 2D photonic crystal slab is successfully fabricated from a GaAs/Al<sub>x</sub>O<sub>y</sub> material system and its intrinsic transmission properties are studied. The crystal slab is shown to have a strong 2D band gap at  $\lambda \sim 1.5 \mu\text{m}$ . Light attenuates as much as  $\sim 5\text{dB}$  per period in the gap, the strongest ever reported for any 2D photonic crystal in optical  $\lambda$ . More importantly, for the first time, the crystal slab is shown to be capable of controlling light fully in all three-dimensions. The lightcone criterion is also experimentally confirmed.

The photonic crystal slab consists of cylindrical holes etched through a thin GaAs slab and partially into a  $1\mu\text{m}$  thick underlying Al<sub>0.9</sub>Ga<sub>0.1</sub>As layer. The holes are arranged in a triangular array, Fig. 1(a), with a lattice constant  $a$  and hole diameter  $d (= 0.6a)$ . Three samples were fabricated with  $a = 400, 430$  and  $460$  nm respectively. The thickness of the GaAs slab is a critical parameter and is chosen to be  $(t=0.5a)$  to create a large photonic band gap [12]. Nanometer scale fabrication of 2D holes is done using a combination of electron-beam lithography and reactive-ion-beam-etching (RIE) processes [14]. The RIE technique allows for etching of GaAs/Al<sub>0.9</sub>Ga<sub>0.1</sub>As materials with a straight sidewall. An integrated waveguide-coupled photonic crystal slab sample is obtained by combining with conventional ridge waveguide. Scanning electron microscope (SEM) top and side view image of it are shown in Figs. 1(b) and 1(c), respectively. The depth of holes is  $\sim 0.5 \mu\text{m}$  and their sidewalls are straight to within  $5^\circ$ . The 2D hole array section is designed to

be a few rows wider than the waveguide to reduce the amount of light leaking around the side edges of photonic-crystal slab. Another reason for the increased width is that the fabricated hole size tends to be more uniform at the middle rows and becomes less controllable near the edges. As a final step in the fabrication, the  $\text{Al}_{0.9}\text{Ga}_{0.1}\text{As}$  layer was wet oxidized into  $\text{Al}_x\text{O}_y$ . The  $\text{Al}_x\text{O}_y$  has a low index value,  $n \sim 1.5$  [15], which helps to confine light in the GaAs slab, better-maintains the symmetry of the guided modes (discussed below).

Figs. 2(a) and 2(b) show the frequency dispersion relation (band structure) of a photonic crystal slab, computed using a full 3D calculation with the sample parameters described above. The frequency  $\omega$  is expressed in units of  $(a/\lambda)$ , and the wavevector is plotted along crystal symmetry axes  $\Gamma$ , M and K, shown in Fig.1 (a). The shaded area represents the lightcone region and connected dots are the guided modes within the slab. The lightcone is a new feature that arises from a full 3D treatment and does not occur in a purely 2D band-structure calculation. Photonic states within such a lightcone extend infinitely into regions outside the slab and are leaky. These are the undesirable radiation modes [13], although they may be useful in out-coupling of light into air [16]. The slope of lightcone boundary is determined by the index value of the underlining  $\text{Al}_x\text{O}_y$  layer.

Below the lightcone boundary, guided modes exist. They cannot couple into air modes due to energy-momentum conservation rules and are localized to the vicinity of the crystal slab. This confinement is analogous to total-internal-reflection and is due to a large index contrast between the GaAs ( $n=3.4$ ) and  $\text{Al}_x\text{O}_y$  layers. Guided modes are classified into TE/even (open circles) and TM/odd (solid circles) states, as in Fig. 2(a), according to the symmetry of the EM wave with respect to reflections through the 2D plane [11]. Strictly speaking, these states are not purely TE or TM polarized, however, these even-like and odd-like states have strong similarities with TE and TM states, respectively, and so we refer to them below as "TE" and "TM". For a perfectly symmetrical 2D slab, TE and TM modes are de-coupled and non-interacting. As shown in Fig.2 (a), a large fundamental TE band gap ( $\omega = 0.263-0.341$ ) exists. Operating within the guided modes, light propagates freely in the 2D plane. In the photonic band gap, on the other hand, light can be strongly confined by a 2D gap and at the same time is index-guided vertically. It is in this sense that light can be fully controlled using a photonic-crystal slab. It must be noted this is not a true 3D band gap [17] due to the small but inevitable radiation loss to the leaky modes in the lightcone region.

For comparison, the dispersion relation for an unoxidized photonic-crystal slab is also shown in Fig. 2(c). In this case, slope of the lightcone,  $c/n$ , is set by the index of  $\text{Al}_{0.9}\text{Ga}_{0.1}\text{As}$  layer,  $n = 2.9$ . A higher  $n$  implies a lower lightcone boundary for the unoxidized crystal slab. Consequently, only the lowest TE and TM band are guided and only a small photonic band gap between the lightcone boundary and the lowest band is expected. The use of a low-index  $\text{Al}_x\text{O}_y$  layer in our 2D slab structure design is essential for obtaining 2D guided modes with sizeable band gaps.

To probe the intrinsic optical properties of a photonic-crystal slab, transmission measurements were carried out in the nearest-neighbor direction,  $\Gamma\text{K}$ . Three diode laser modulates were used as the light source. The laser output has a well-defined Gaussian profile, and is tunable from  $\lambda = 1290$  to  $1350$  nm,  $\lambda = 1525$  to  $1595$  nm and  $\lambda = 1625$  to  $1680$  nm. This tuning range allows us to simultaneously probe the band gaps, band edges and guided

## **DISCLAIMER**

This report was prepared as an account of work sponsored by an agency of the United States Government. Neither the United States Government nor any agency thereof, nor any of their employees, make any warranty, express or implied, or assumes any legal liability or responsibility for the accuracy, completeness, or usefulness of any information, apparatus, product, or process disclosed, or represents that its use would not infringe privately owned rights. Reference herein to any specific commercial product, process, or service by trade name, trademark, manufacturer, or otherwise does not necessarily constitute or imply its endorsement, recommendation, or favoring by the United States Government or any agency thereof. The views and opinions of authors expressed herein do not necessarily state or reflect those of the United States Government or any agency thereof.

## **DISCLAIMER**

**Portions of this document may be illegible in electronic image products. Images are produced from the best available original document.**

modes of the crystal slab. For the polarization study, a polarization rotator was used to produce pure TE and TM input light (which couple to even and odd guided modes respectively). To couple laser light into and out of a ridge waveguide, a pair of aspheric lenses with a high numerical aperture (NA=0.4) was used. The output light is then split and fed into a calibrated InGaAs photo-detector and an infrared (IR) camera respectively. For precise optical alignment, the sample and lenses are mounted to a five-axis moving stage, which has a movement precision of better than 100 nm.

To obtain reliable transmittance data, modal profile of the transmitted light must be carefully examined. In our experimental configuration, Fig. 1(b), transmitted signal is a combined effect of light coupling from (i) the input waveguide mode into (ii) the photonic-crystal state and then back to (iii) the output waveguide mode. If laser light is well focused into the input waveguide and the crystal slab does not strongly scatter light, output signal is a well-defined Gaussian-shape waveguide mode. On the other hand, if focus is off and laser light is coupled, instead, into the undesired air mode or the substrate leaky mode, output signal is typically broad and scattered in shape. An IR imaging camera at the output end is a useful tool for checking modal profile. Fig.3 (a) shows an IR image of a TM light of  $\lambda = 1550$  nm transmitted through a nine-period 2D crystal sample ( $a = 460$  nm). The mode is bright and well defined. Its intensity profile, shown at the bottom as a dashed line, follows a Gaussian-like. The same measurement is repeated with TE light and the resulting image is shown in Fig. 3(b). The image is not as bright, but its profile remains a Gaussian-shape. The observed Gaussian profile suggests that the output signal is a true measure of waveguide-crystal interaction. Also, the much weaker TE intensity suggests the existence of a TE gap at  $\lambda = 1550$  nm.

To find absolute transmittance of a 2D crystal, a reference transmission is taken from an identical waveguide with no 2D crystal built in the middle section. By normalizing transmission signals with this reference transmission, absolute transmittance is obtained. This procedure eliminates external uncertainties associated with reflection at waveguide-crystal interfaces and free space-to-waveguide coupling efficiency and allows for an absolute determination of intrinsic transmittance of the crystal slab.

In Fig. 4, the TM absolute transmittance versus the number of period ( $N$ ) of the hole array ( $a = 460$  nm) is plotted as solid squares. The laser wavelength is  $\lambda = 1550$  nm, and the corresponding  $\omega (= a/\lambda)$  is 0.297. The transmittance is high,  $(88 \pm 7)\%$ , and is independent of  $N$ . The high transmittance shows that TM light is well-guided within the crystal slab, as predicted by the band structure calculation shown in Fig.2(b). This observation confirms the prediction that, under the lightcone, light is guided in the crystal slab and vertical leakage loss is negligible. Additionally, this data shows that out-of-plane scattering due to fabrication imperfection is not important for our sample.

At  $\omega = 0.297$ , TE input light is strongly attenuated and, quite surprisingly, is also slowly converted to a TM polarization. In Fig.4, the total and TE transmitted light is plotted as open and solid circles, respectively. The data from TE transmitted light will be discussed here first and the polarization conversion issue will be addressed in a later paragraph. The TE transmittance drops exponentially from 50% at  $N=1$ , to  $\sim 0.2\%$  at  $N=5$ , and eventually saturates at  $\sim 6 \times 10^{-4}$ . The observed exponential dependence shows that, at  $\omega = 0.297$ , the TE mode is in the photonic band gap regime. This result agrees with the

prediction presented in Fig. 2(a). As this TE mode is well below light-cone, vertical light leakage within the crystal is negligible. Thus, the observed absolute transmittance is a true measure of light attenuation in the 2D crystal slab. The attenuation capability of this photonic band gap is strong. Light attenuates by a factor of 10, for every two-periods it traverses in the crystal slab, i.e.  $\sim 5\text{dB}$  per period, the strongest ever reported in any 2D photonic crystals at optical  $\lambda$ .

To explore dispersion of a photonic-crystal slab, nine experimental data sets were taken covering  $\omega$  from 0.24 to 0.35. This task is accomplished by scanning three laser modulates through three different samples with  $a = 400\text{ nm}$  (red dots),  $430\text{ nm}$  (green dots) and  $460\text{ nm}$  (blue dots), respectively. The thickness of each sample is maintained at  $0.5a$ . In Fig.5, the measured TE transmission spectrum is plotted in a semi-log scale. The solid and open dots represent TE and total transmitted data, respectively. A theoretical curve (solid line) is also shown, which agrees well with the experimental data. The theoretical transmission calculation were performed using 3D finite difference time-domain simulations with 10 pixels per  $a$  and absorbing boundary conditions. The slightly larger observed band gap,  $\sim 8\%$ , may be due to small uncertainties in fabrication parameters, the hole size and lattice constant. In the band gap, transmittance as low as  $\sim 2 \times 10^{-4}$  is observed. At the lower band edge,  $\omega \sim 0.25$ , transmittance increases from  $2 \times 10^{-4}$  to unity over a small  $\Delta\omega \sim 0.02$ , a four order of magnitude rise. The upper and lower TE band edges occur at  $\omega_1 \sim 0.34$  and  $\omega_2 \sim 0.25$ , respectively, yielding a large gap-to-midgap ratio, 30%. Within this band gap, light can be strongly confined by the 2D gap and index-guided vertically. Experimental demonstration of such a 3D control of light is a pre-requisite for realizing novel photonic-crystal devices such as thresholdless lasers [1].

The polarization conversion mentioned in Fig. 4 may be attributed to symmetry breaking in the slab structure. In our sample, the upper cladding is essentially air, whereas the lower cladding is a thick  $1\mu\text{m Al}_x\text{O}_y$  layer. This asymmetry [11] introduces a weak coupling between the TE and TM modes in the waveguides and the opposite-symmetry modes in the crystal. At  $\omega = 0.297$ , while TE light is attenuated due to the TE gap, TM light is free to propagate and should remain roughly constant. Thus for small  $N$  ( $<3$ ) in Fig.4, TE light dominates and its intensity close to that of total transmitted light. For  $3 < N < 5$ , the converted TM intensity increases yet TE light continues to drop, leading to a large difference between TE and the total transmitted light. For  $N > 5$ , TM polarization dominates the total transmitted light and its intensity remains a constant as it is a guided mode. At this point, a back-conversion from TM to TE becomes significant, leading to a nearly constant TE light intensity. The TE to TM ratio here of about 0.05 is a measure of TE/TM mode conversion efficiency. This TE/TM conversion process contributes to light leakage and will limit the attenuating efficiency of a TE gap. Such leakage, however, may be eliminated through a symmetrical slab structure design ( $\text{Al}_x\text{O}_y$  above and below).

This work realizes a new class of photonic-crystal structure that is capable of fully controlling light in optical  $\lambda$ . These important features originate from the use of an optimally designed thin 2D slab and a low-index underlying  $\text{Al}_x\text{O}_y$  layer. This demonstration sets a new foundation for 2D crystal structures and will impact a wide class of planar-photonic-circuits components and their integration. Possible applications include low loss in-plane waveguide bends [18], waveguide crossings for integrated-optical-circuit applications

[19], and photonic tunneling [20] for wavelength division multiplexer/de-multiplexer applications.

## References

1. Yablonovitch, E., Photonic band-gap structures. *J. Opt. Soc. Am. B* 10, 283-295 (1993).
2. John, S., Localization of light, *Phys. Today*, 32-40, May 1991.
3. Ho, K. et al., Photonic band gaps in three dimensions: new layer-by-layer periodic structures, *Solid State Comm.* 89, 413-416 (1994).
4. Ozbay, E. et al., Measurement of three-dimensional photonic band gap in a crystal structure made of dielectric rods, *Phys. Rev. B* 50, 1945-1948 (1994).
5. Lin, S.Y. et al., A three-dimensional photonic crystal operating at infrared wavelengths, *Nature*, 394 251-253 (1998).
6. For a general reference, please see *Photonic band gaps and localization*, edited by C.M. Soukoulis, NATO ASI Series (Plenum Press, New York, 1993). And Joannopoulos, J., Meade, R., & Winn, J., *Photonic Crystals*, (Princeton, New York, 1995).
7. Robertson, W.M. et al., Measurement of Photonic Band Structure in a Two-Dimensional Periodic Dielectric Array, *Phys. Rev. Lett.* 68 2023-2026 (1992).
8. Lin, S.Y. et al., Investigation of absolute photonic band gaps in two-dimensional dielectric structures, *J. Modern Optics*. Vol. 41, 385-393 (1994).
9. Gruning, U. and Lehmann, V. Two-dimensional infrared photonic crystal based on microporous silicon, *Thin Solid Films*, Vol. 276, 151-154 (1996). And Rosenberg, A. et al., Near-infrared two-dimensional photonic band gap materials, *Optics Lett.* , Vol. 21, 830-832 (1996).
10. Krauss, T.F. et al., Two-dimensional photonic band gap structures operating at near-infrared wavelengths, *Nature*, Vol. 383, 699-702 (1996). And Labilloy, D. et al., Quantitative Measurement of transmission, reflection, and diffraction of Two-Dimensional Photonic Band Gap Structures at Near-Infrared Wavelengths, *Phys. Rev. Lett.* 79, 4147 (1997).
11. Villeneuve, P.R. et al. Three-dimensional photonic confinement in photonic crystals of low-dimensional periodicity, *IEE Proc. Optoelec.*, vol. 145, 384-390 (1998).
12. Johnson, S.G. et al., Guided modes in photonic crystal slabs, *Phys. Rev. B* 60 5751-5758 (1999).
13. Kanskar, et al., Observation of leaky slab modes in an air-bridged semiconductor waveguide with a two-dimensional photonic lattice, *Appl. Phys. Lett.* 70, 1438 (1997).
14. Wendt, et al., Nano-fabrication of photonic lattice structures in GaAs/AlGaAs, *J. Vac. Sci. & Tech. B* 11, 2637 (1993).
15. Kish, et al., Planar native-oxide index-guided in AlGaAs/GaAs quantum well heterostructure lasers, *Appl. Phys. Lett.* . 59, 1755(1991).
16. Fan, S. et al., High extraction efficiency of spontaneous emission from slabs of photonic crystals, *Phys. Rev. Lett.* Vol.78, 3294-3297 (1997).

17. Fleming, J.G. and Lin. S.Y., Three-dimensional photonic crystal with a stop band from 1.35 to 1.95  $\mu\text{m}$ , *Optics Lett.*, 24, 49 (1999).
18. Lin, S.Y. et al., Experimental Demonstration of Guiding and Bending of Electromagnet Waves in a Photonic Crystal, *Science* 282, 274-276 (1998).
19. Johnson, S. et al., Elimination of cross talk in waveguide intersections, *Optics Lett.* 23, 1855-1857 (1998).
20. Fan, S. et al., Channel drop tunneling through localized states, *Phys. Rev. Lett.* 772, 3787 (1998).

**Acknowledgments** The work at Sandia National Laboratories is supported through DOE. Sandia is a multiprogram laboratory operated by Sandia Corporation, a Lockheed Martin Company, for the United States Department of Energy. The work at Massachusetts Institute of Technology is supported by MRSEC and by NSF.

Correspondence and requests for materials should be addressed to S.Y.L. (email: slin@sandia.gov)



## Figure Caption

Fig.1(a) A schematic of the 2D triangular array and major crystal symmetry directions; (b) SEM top view of a nine periods 2D photonic crystal slab, connected with input/output waveguides along  $\Gamma K$  direction; (c) a SEM cross-sectional view of the etched hole array, showing cylindrical holes with a near perfect straight side-wall.

Fig. 2 Computed dispersion of 2D photonic crystal slab structures assuming refractive index of GaAs is  $n=3.4$ ,  $d=0.6a$  and  $t=0.5a$ . The top cladding layer is air and the bottom cladding layer is either  $\text{Al}_x\text{O}_y$  ( $n=1.5$ , Fig. 2a and 2b) or  $\text{Al}_{0.9}\text{Ga}_{0.1}\text{As}$  ( $n=2.9$ , Fig.2c). The shaded area is the light-cone region. The 2D guided modes are classified into TM (solid dots) and TE (open dots).

Fig. 3(a) and (b) TM and TE infrared images of light at the waveguide output facet of a 2D crystal slab sample. The input laser wavelength is  $\lambda=1550$  nm, corresponding to a reduced frequency  $\omega=0.297$ . Both TM and TE modal profiles are Gaussian-like. The TM light is brighter as it belongs to a guided mode. The TE light is much weaker and is in the photonic band gap spectral regime.

Fig. 4 Absolute transmittance ( $T$ ) versus number of periods ( $N$ ) for a series of 2D crystal samples. The laser wavelength is  $\lambda=1550$  nm and  $\omega$  is 0.297. The transmittance for TM input (solid squares) is high and independent of  $N$ , suggesting that light is well confined within the 2D slab and propagates freely in the 2D plane. For TE input, transmitted light contains TE and TM components, both attenuating exponentially as a function of  $N$ . For TE output, the attenuation is  $\sim 5\text{dB}$  per period, the strongest ever reported in any 2D crystals in optical  $\lambda$ .

Fig. 5 Absolute transmittance versus  $\omega$  for TE input light. The solid line is theoretical curve. The solid and open dots are measured output signal containing TE- and both polarizations, respectively. The TE gap is strong, with a minimum  $T$  as low as  $2 \times 10^{-4}$ . TE band edges are clearly observed as well as a small portion of the guided band with a near 100% transmittance.

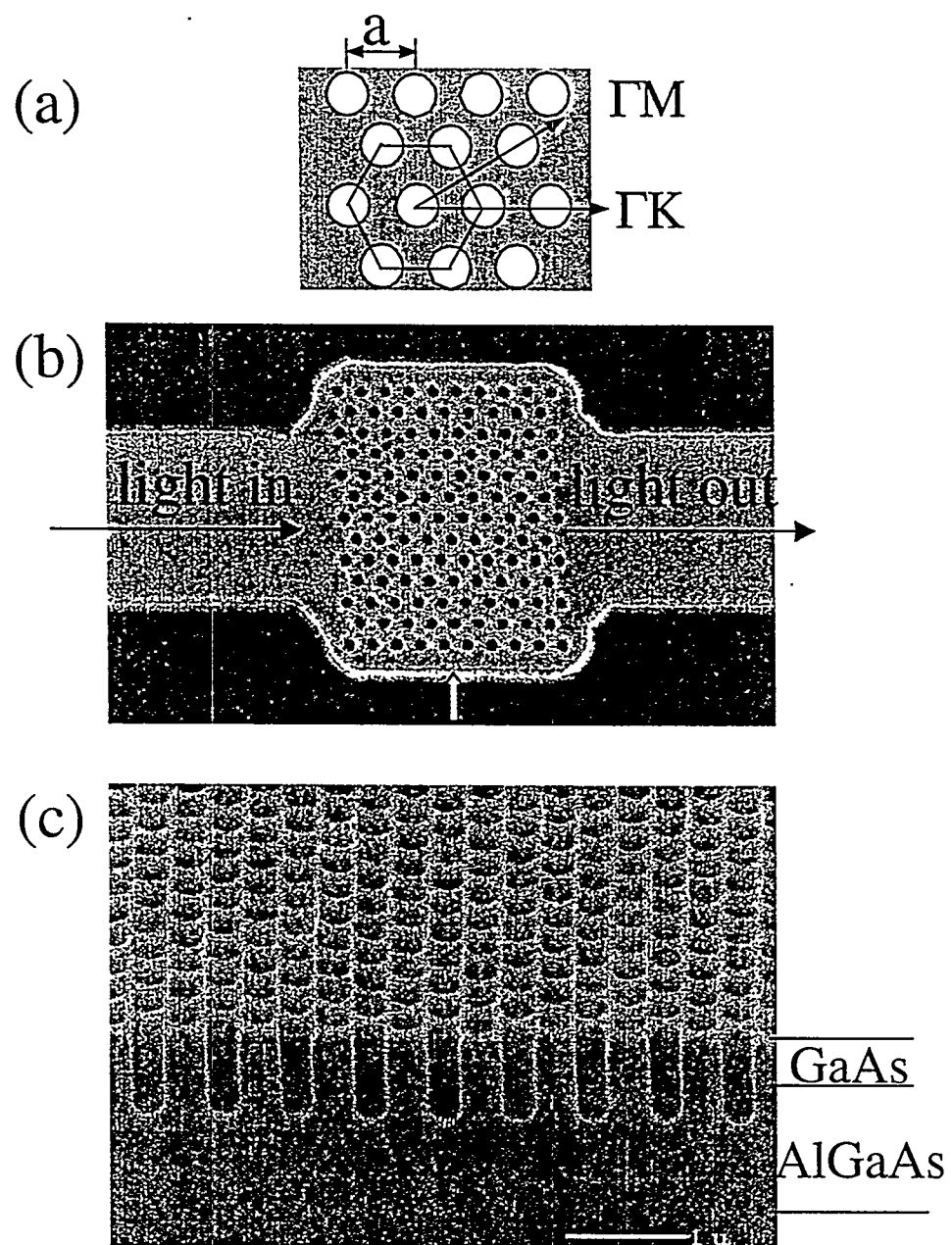


Fig. 1

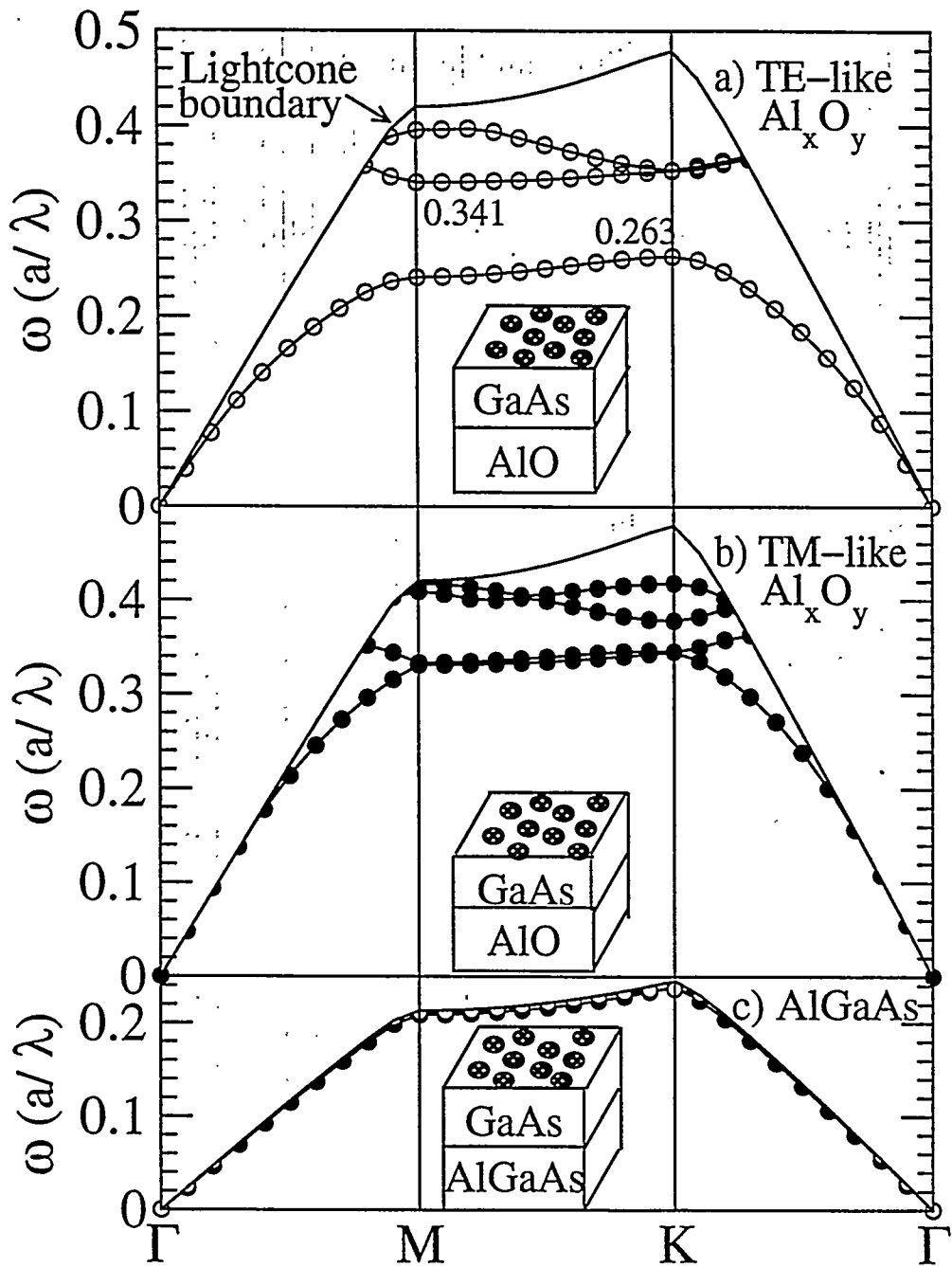


Fig. 2

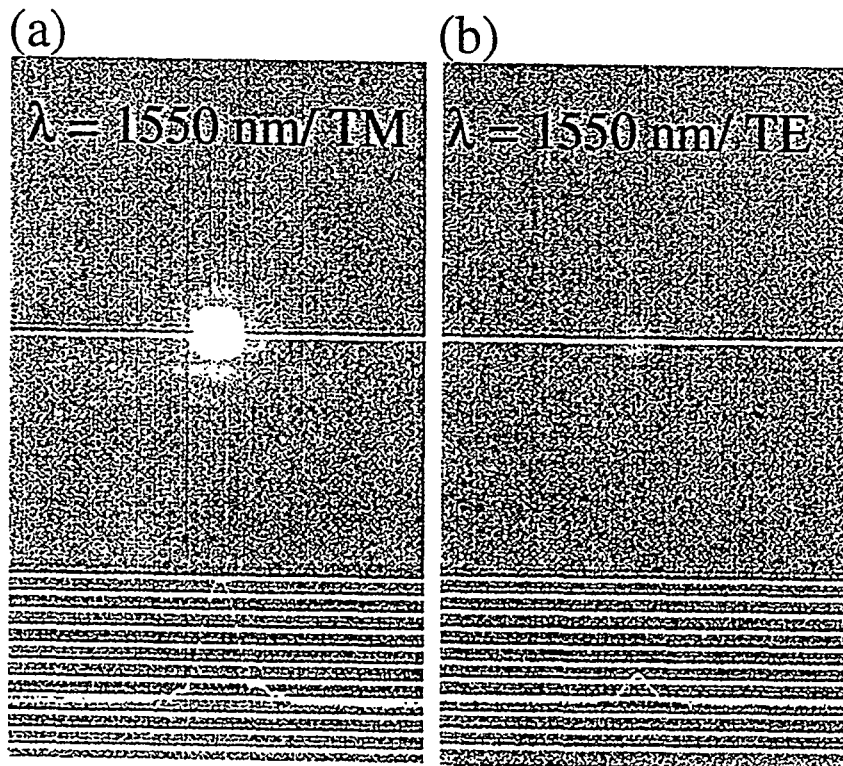


Fig.3

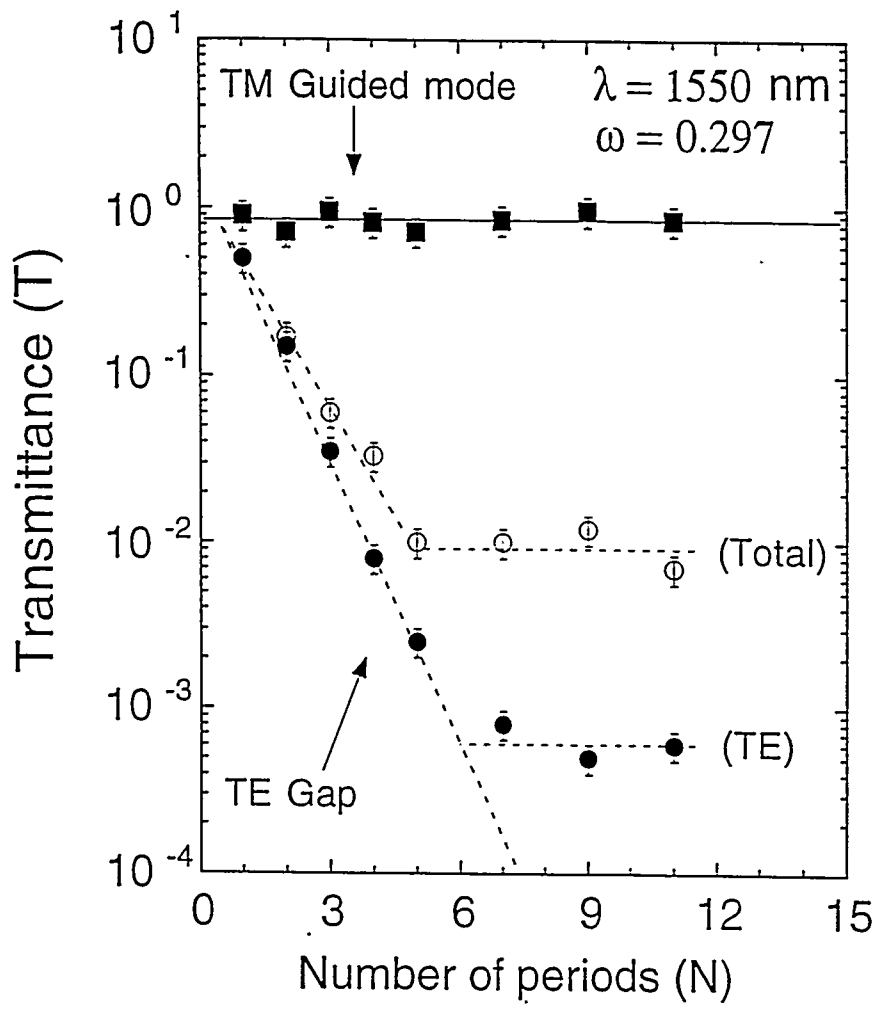


Fig. 4

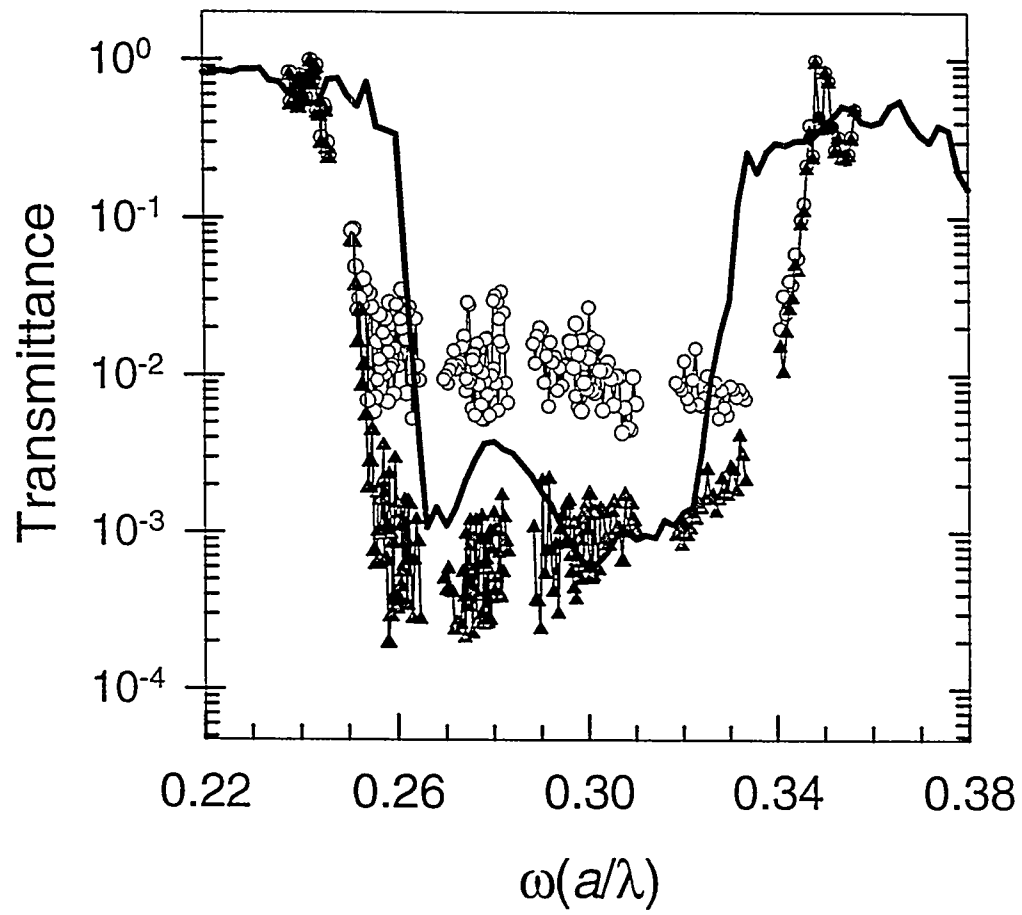


Fig. 5